Proceedings of the 2021 IEEE International
Conference on Intelligence and Safety for Robotics
Nagoya, Japan, March 4-6, 2021

A Safety Joint with Passive Compliant and Manual Override Mechanisms for Medical Robotics

Jia Zheng, Shuangyi Wang, James Housden, Zeng-Guang Hou, Davinder Singh, Kawal Rhode

Abstract— **Force and collision control is a primary concern to guarantee the safe use of medical robots as such systems normally need to interact with clinicians and patients, while at the same time cooperate with other devices. Among different strategies, passive features working with intrinsically safety components are treated as one of the most effective approaches and therefore deserve in-depth study. In this study, we focus on the design of a novel back-drivable safety joint that incorporates a torque limiter with passive compliance and a manual override mechanism to disconnect the robotic joint from its drive train. The design and working principle of the proposed joint are explained, followed by the mathematical analysis of its performance and the impacts of parameters. An example of the design was manufactured and tested experimentally to validate the working concepts. It is concluded that the proposed multi-functional safety joint provides more versatility and customization to the design of bespoke medical robots and would limit the maximum torque that can be exserted onto the patient, allow the clinician to push the joint back, and enable the operator to switch back to manual override.**

I. Introduction

Safety is one of the important issues in designing a medical robot as the system normally needs to cooperate and interact with both clinicians and patients [1], e.g. surgical robots working collaboratively with the surgeon, rehabilitation robots assisting desirable motions of the patient, and palpation robots exserting force on patient's body. In this close operating proximity, force and collision controls become crucial. In addition to human factors, operating rooms are cluttered with many other medical systems that may collide with the robot. Therefore, special considerations for force and collision managements may also be necessary to guarantee the safe use of the other co-existing systems.

Considering possible strategies, force control methods based on various sensing and programming techniques are widely investigated with extensive literatures to introduce active compliance to the robot. To do so, reactive planning and actuation would be activated in the presence of detecting and localizing excessive force or workspace sharing. However, because of the possible failures of sensing, computing, and electrical systems, there still exists the possibility that could lead to the injuries of the clinician and patient working alongside robots. Therefore, intrinsic components and passive features employed in medical robotic systems would greatly improve the design reliability. Among the possible approaches, limitation of actuator's power to satisfy only the required tasks could be one of the most basic considerations although the expected force may still be harmful. The use of high reduction gears, e.g. worm-gear mechanism or harmonic drives reduces the robot's velocity and prevents the robot from collapsing although this may end up in non-back-drivable structures. Moreover, magnetic connection or torque limiters can be included to enable the disconnection of certain structures, e.g. the collar linking the endoscope and the robotic arm can be disconnected on AESOP [2], the following link stops moving while the motor shaft still rotates when there is a collision occurring on Neurobot [3].

With the combined use of special mechanical mechanisms and elastic components, passive compliance with customized structures can also be achievable that the joint will allow deviations from its own equilibrium position, when the applied external force exceeds certain threshold. Example of such works can be found in [4] where a safe joint mechanism that consists of linear springs and a slider-crank mechanism is proposed. Besides, a safe and compact joint with the use of rollers and pockets to form a torque limiter was introduced in [5] and a threshold-adjustable torque clutch that comprises spring, cam, and lever was introduced in [6].

Based on our initial work introduced in [7], this study presents a design containing a passive mechanical clutch which limits the maximum amount of torque exerted by the joint and a manual drive engagement and disengagement method to disconnect the robotic joint from its drive train. The design has been improved compared with the previous work, which resolves the problem that the limiting torque is susceptible to the deformation of the clutch case. Additionally, the new design has two clutches collocated in one joint, enabling the joint not only to limit the torque but also allow the joint to be freely moved away from the patient independently from any electrical powering system or control software. To introduce the design, the proposed mechanism and working principle are first described. The performance is then analyzed mathematically with a parameter optimization strategy presented to highlight the customization approach. An implementation example is then presented, followed by the conclusion of the work.

II. Design and Working Principles

The proposed safety joint consists of two clutches, i.e. manual override and torque limiting clutches. The manual override clutch (Fig. 1) makes use of the mechanism of a

* This work was funded by the Wellcome Trust IEH Award (102431) and National Natural Science Foundation of China (NSFC) (62003339). The authors acknowledged the supports from the Wellcome/EPSRC Centre for Medical Engineering (WT203148/Z/16/Z).

Corresponding author: Shuangyi Wang (shuangyi.wang@ia.ac.cn).

J. Zheng is with the School of General Engineering, Beihang University, Beijing 100191, China.

S. Wang and Z. Hou are with the State Key Laboratory of Management and Control for Complex Systems, Institute of Automation, Chinese Academy of Sciences, Beijing 100190, China.

J. Housden and K. Rhode are with the School of Biomedical Engineering and Imaging Sciences, King's College London, London SE1 7EH, UK.

D. Singh is with the Xtronics, Ltd., Gravesend, Kent DA12 2AD, UK.

2021 IEEE International Conference on Intelligence and Safety for Robotics (ISR) | 978-1-6654-3862-9/21/$31.00 ©2021 IEEE | DOI: 10.1109/ISR50024.2021.9419379

mechanical latch. Under normal working circumstances, the latch allows the worm and gear to be engaged with the catch clicked in, and power can be transmitted from the drive train, i.e. worm to gear in this example. When necessary, e.g. the actuated link would need to be moved quickly out of the way from interaction with people or if the system is malfunctioning or running out of power, pushing the handle on the joint will cause the worm-gear disengagement. During this process, the handle would interact with the catch and serves as the strike. After pushing the handle, the spring-loaded catch clip will rotate, as indicated in Fig. 2. The rotation of the catch clip will push against the handle, causing the entire catch case to rotate around the countershaft (Fig. 1). Note that handle is fixed to the catch case. The catch case and the worm gear are mounted on the same shaft and rotate together around the countershaft. Therefore, the movement of the catch case will cause the disengagement of the worm and gear. Pushing the handle again will reset the engagement of the worm and worm gear.

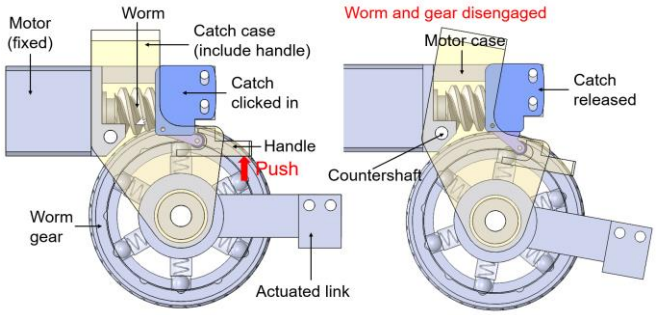

Fig. 1. Schematic representation to illustrate the working mechanism of the manual override clutch. Pressing the handle will trigger the clutch, causing the catch to be released. Pressing the handle again will reset the clutch.

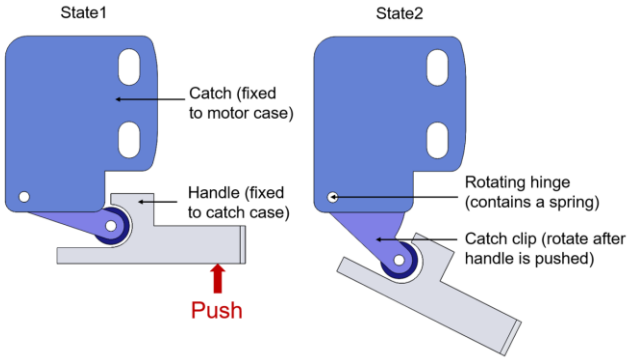

Fig. 2. Schematic representation to illustrate the working mechanism of the manual override clutch catch in detail. Pressing the handle will cause the catch clip to rotate (State 1 to State 2) and pressing the handle again will restore the handle to the initial state (State 2 to State 1). Note that the handle is fixed to the catch case.

The torque limiting clutch makes use of ball-spring pairs that are inserted into the detent holes, with the radius of the ball denoted as R and the spring constant as k. A detailed illustration of the torque limiting clutch is shown in Fig. 3. When not triggered, the inner and the outer clutches are tightly engaged, with the ball held by a preloaded spring compressed by the clutch cover. The preload is denoted as P_0. This means that the outer and the inner clutches will rotate at the same speed. The details of the ball-spring detent are shown in Fig. 4.

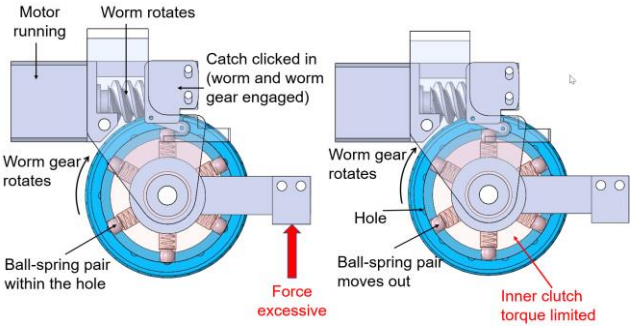

Fig. 3. Schematic representation to illustrate the working mechanism of the torque limiting clutch. Excessive force will trigger the clutch.

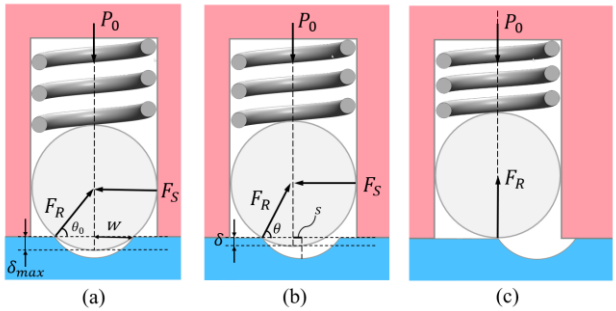

Fig. 4. Schematic representation showing the details of the ball-spring detent. "s" corresponds to the displacement caused by the horizontal shear force. (a) is the initial state. Excessive torque causes the ball to move out of the detent, going from state (a) to (b) to (c).

When excessive torque is exserted on the joint, the balls will be pushed out of their respective detent holes, which stops the transmission from the outer to the inner clutch. The amount of horizontal movement of the ball in this process is denoted as s. A horizontal shear force F_S is developed between the inner clutch and the ball. The detent hole is a conical notch, with a radius of w. There is a reaction force between the edge of the detent hole and the ball, which is denoted as F_R, as is shown in Fig. 4. If the torque decreases, the balls will re-engage into the next detent holes, and the joint will be reset again. otherwise, the balls will keep rotating together and there will be no transmission between the outer and inner clutch.

III. Performance Analysis and Parameter Selection

This section models the performance of the torque limiting clutch mathematically, analyze the impacts of the parameters, and propose an optimization strategy. The parameters are indicated in Fig. 4. The variable θ is the angle between the horizontal plane and the reaction force F_R:

$$\theta = \arccos\left(\frac{w-s}{R}\right). \tag{1}$$

The variable δ gives the vertical displacement of the ball from the initial position to the transitional position:

$$\delta = R - \sqrt{R^2 - (w-s)^2} = R - R\sin(\theta). \tag{2}$$

The maximum vertical displacement of the ball is:

$$\delta_{\max} = R - R\sin(\theta_0), \tag{3}$$

where θ_0 is the initial angle (Fig. 4 (a)). The vertical force F_V generated by the force resulting from the compression of the spring due to the movement of the ball and the preloaded force generated from the clutch is:

$$F_V = k(\delta_{\max} - \delta) + P_0 = kR(\sin(\theta) - \sin(\theta_0)) + P_0. \tag{4}$$

The horizontal shear force developed during the process is:

$$F_S = \frac{F_V}{\tan(\theta)} = \frac{kR(\sin(\theta) - \sin(\theta_0)) + P_0}{\tan(\theta)}. \tag{5}$$

Once the system is set, the parameters k, R, θ_0, and P_0 will be fixed. To design a torque limiting clutch, the maximum allowable shear force that can be applied to the clutch should be known based on its intended application.

Differentiate F_S with respect to θ:

$$\frac{\partial F_s}{\partial \theta} = \frac{-kR(\sin^3(\theta) - \sin(\theta_0)) - P_0}{\sin^2(\theta)}, \tag{6}$$

where $\theta \in (\theta_0, 90^\circ)$, therefore, $\sin(\theta) > 0$. To determine the sign of $\frac{\partial F_s}{\partial \theta}$, analyze $\frac{-kR(\sin^3(\theta) - \sin(\theta_0)) - P_0}{\sin^2(\theta)} = 0$, which is equivalent to

$$\sin(\theta) = \sqrt[3]{\sin(\theta_0) - \frac{P_0}{kR}}. \tag{7}$$

Let $A := \sqrt[3]{\sin(\theta_0) - \frac{P_0}{kR}}$ Using the first derivative test, if $A \le \sin(\theta_0)$, F_s reaches the maximum at $\theta_m = \theta_0$; if $A \in (\sin(\theta_0), 1)$, F_s reaches the maximum at $\theta_m = \arcsin(A)$. This relation is shown in Fig. 5. Note that A is always less than 1, because $\sin(\theta_0) < 1$.

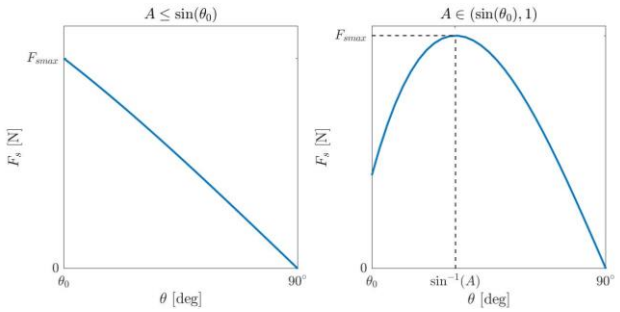

Fig. 5. Plot showing the maximum of the horizontal shear force F_{smax}.

The maximum horizontal shear force is

$$F_{smax} = \frac{kR(\sin(\theta_m) - \sin(\theta_0)) + P_0}{\tan(\theta_m)} = f_1(k, \Delta l, R, w), \tag{8}$$

where Δl is the displacement of the spring and from Hooke's law, $P_0 = k\Delta l$. F_{smax} is a function of $k, \Delta l, R, w$.

The overall limited torque T for the clutch is:

$$T = nF_{S\,max}h = f_2(n, h, k, \Delta l, R, w), \tag{9}$$

where n is the number of ball-spring pair and h is the distance between the center of the ball to the center of the inner clutch. Based on the above analysis, a parameter selection strategy is summarized in Fig. 6.

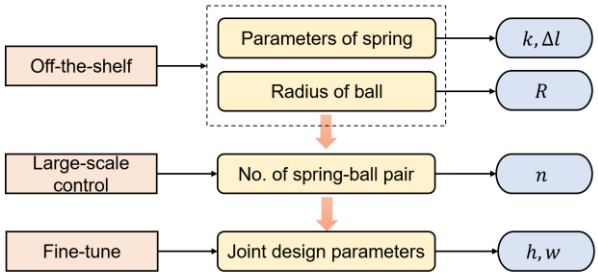

Fig. 6. Flow diagram showing the process of parameter selection.

IV. Implementation Example

Based on the working principle presented in Section II and the parameter selection strategy described in Section III, this section aims to show an implementation example. Eq. (8) and (9) indicate the maximum shear force and torque allowed by the clutch, which provides the quantitative guidance to the design of the clutch. As a case study, the targeting torque to be limited was set at 941N·mm, which would result in the maximum allowable force 14.43N at the distal end with a 65.2mm-length test link designed and assembled. To select the appropriate parameters, the parameters of spring-ball pairs were first decided and the joint design parameters were then optimized based on Eq. (9). The resulted parameters are summarized in Table 1 and the manufactured safety joint is shown in Fig. 7(a). The plastic parts were 3D printed using Polylactic acid (PLA). The catch and the motor are both standard off-the-shelf components that can be easily bought from the market.

TABLE I. SUMMARY OF THE IMPLEMENTED SAFETY JOINT

Theatrical threshold/ Torque (N·mm)	Parameters of the implemented safety joint					
	n	*h*/ mm	*R*/ mm	*k*/ (N·mm)	*Δl*/ mm	*w*/ mm
941	6	33.7	4	2	4.03	2

To validate the performance of the manual override clutch, the handle on the design was manually pressed to disengage the drive and re-pressed to re-engage. This has been tested repeatedly and it is observed that the manual override clutch can successfully work as expected. To validate the performance of the torque limiting clutch, measuring side of a commercial force sensor (JHBM-H3, JNSensor, Anhui, China) was mounted onto the distal end of the joint. The design was fixed onto the table with a clamp and its distal link was manually pushed on the other side of the force sensor (Fig. 7(b)). The maximum force was recorded during the process. This experiment was repeated six times. Note that clamping the catch case or clamping the motor produced the same result in this experiment, since the catch is clicked in and the catch

case cannot rotate relative to the motor. Compared with the expected triggering force (14.43N), the average tested value is 14.42N, with a standard deviation of 0.63. The mean absolute error (MAE) is found to be 0.002, and the coefficient of variation is 4%.

Fig. 7. (a) Implementation of the proposed design and (b) experimental setup to measure the triggering torque.

V. Conclusion

This study introduced a novel back-drivable safety joint that incorporates a torque limiter with passive compliance and a manual override mechanism to disconnect the robotic joint from its drive train. The design, the performance analysis, and an implementation example were introduced and the successful working of the design was further validated experimentally. It is therefore concluded that the proposed multi-functional joint could provide more versatility and customization to the design of bespoke medical robots as it can serve as a torque limiter, induce passive compliance, and provide manual override. The limitation of the current design is that the transmission between the balls and the outer clutch is not smooth enough, which may also be the main reason to account for the difference between the designed and measured triggering torque. This will be improved in our future work.

References

[1] M. Y. Jung, R. H. Taylor and P. Kazanzides, "Safety Design View: A conceptual framework for systematic understanding of safety features of medical robot systems," in *Proc. 2014 IEEE Int. Conf. Robot. Autom.*, pp. 1883–1888.

[2] C.-A. Nathan, V. Chakradeo, K. Malhotra, H. Dagostino, and R. Patwardhan, "The Voice-Controlled Robotic Assist Scope Holder AESOP for the Endoscopic Approach to the Sella," *Skull Base*, vol. 16, no. 03, pp. 123–131, Aug. 2006.

[3] G. Duchemin, P. Poignet, E. Dombre and F. Peirrot, "Medically safe and sound [human-friendly robot dependability]," *IEEE Robot. Autom. Lett.*, vol. 11, no. 2, pp. 46–55, June 2004.

[4] J.-J. Park, J.-B. Song, and H.-S. Kim, "Safe joint mechanism based on passive compliance for collision safety," in *Recent Progress in Robotics: Viable Robotic Service to Human*. S. Lee, I.-H. Suh, M.-S. Kim, Berlin, Germany: Springer, 2007, pp. 49–61.

[5] X. Guo *et al*., "A torque limiter for safe joint applied to humanoid robots against falling damage," in *Proc.* 2015 *IEEE Int. Conf. Robot. Biomim*., pp. 2454–2459.

[6] D.-E. Choi, W. Lee, S. H. Hong, S.-C. Kang, H. Lee, and C.-H. Cho, "Design of safe joint with variable threshold torque," *Int. J. Precis. Eng. Manuf.*, vol. 15, no. 12, pp. 2507–2512, Dec. 2014.

[7] S. Wang *et al*., "Analysis of a customized clutch joint designed for the safety management of an ultrasound robot," *Appl. Sci.*, vol. 9, no. 9, p. 1900, May 2019.